Loss of Second-Ballooning Stability in Three-Dimensional Equilibria

C. C. Hegna[1] and S. R. Hudson[2]

[1]*Departments of Physics and Engineering Physics, University of Wisconsin, Madison, Wisconsin 53706-1687*
[2]*Princeton Plasma Physics Laboratory, Princeton, New Jersey 08543*

(Received 13 March 2001; published 27 June 2001)

The effect of three-dimensional geometry on the stability boundaries of ideal ballooning modes is investigated. In particular, the relationship between the symmetry properties of the local shear and the magnetic curvature is addressed for quasisymmetric configurations. The presence of symmetry breaking terms in the local shear can produce localized ballooning instabilities in regions of small average magnetic shear which lower first-ballooning stability thresholds and can potentially eliminate the second stability regime.

DOI: 10.1103/PhysRevLett.87.035001 PACS numbers: 52.35.Py, 52.30.–q, 52.55.Dy, 52.55.Hc

Ballooning instabilities are short wavelength pressure driven ideal magnetohydrodynamic (MHD) modes [1] that limit plasma performance. For the stellarator class of magnetic confinement devices, ballooning stability criteria are often the most restrictive. Ballooning instabilities are driven by a pressure gradient in a region of configuration space with unfavorable magnetic field curvature. Since curvature varies on the magnetic surfaces of toroidal confinement devices, the eigenmode structure tends to localize on the magnetic surface to facilitate access to the free energy source. Instability ensues when the destabilizing pressure/curvature drive is more virulent than stabilizing field line bending energy which is influenced by the local shear of the magnetic field line. The geometry of the magnetic field lines is important in describing the eigenmode structure and associated instability properties. Prior work [2] led to important insights into the nature of ballooning stability in tokamak configurations. A number of authors looked at the stability properties of specific stellarator configurations [3,4], but it is difficult to draw general conclusions from these studies about the nature of MHD ballooning stability in three-dimensional configurations. In this paper, we attempt to understand some of the generic physics of ballooning stability relating to the role of three-dimensional (3D) magnetic geometry.

A particularly important result of ballooning stability studies in axisymmetric configurations is the discovery of the second stability regime [2,5]. A key element in understanding the physics of the second stability regime is the role of the local shear [2]. In toroidal configurations, the local shear is influenced by pressure driven Pfirsch-Schlüter effects. To minimize the stabilizing effect of field line bending, the most unstable ballooning mode eigenfunctions reside in regions of small local shear. For the small pressure gradient, the low shear region lies on the large major radius side where the curvature is unfavorable. At higher pressure gradient, the region of small local shear moves away from the bad curvature region towards a region on the magnetic surface with favorable curvature. Consequently, at sufficiently high enough pressure gradient, the pressure modification of the stabilizing field line bending energy overcomes the destabilizing curvature drive, and the ballooning mode is stabilized. Typically, this second stability regime is limited to regions with small averaged magnetic shear; however, axisymmetric shaping and the aspect ratio affect quantitative estimates of the stability boundary. Consequently, tokamaks with weak or reversed magnetic shear have very good ballooning stability properties. As is shown in the following, the presence of symmetry breaking effects can have a dramatic impact on the "second stable" region.

The difficult aspect of appreciating the role of three-dimensional shaping on ballooning instability is the generation of the equilibria themselves since there is no general prescription for the complete specification of 3D magnetostatic equilibria in a toroidal domain with concentric toroidal flux surfaces (surfaces upon which magnetic field lines lie). However, a method was developed [6] to generate a sequence of three-dimensional equilibria in a region localized to a magnetic surface; this generalizes previous work on local solutions to the Grad-Shafranov equation on asymmetric flux surfaces [2,7,8]. By application of this technique, one is able to calculate stability boundaries for modes localized to magnetic surfaces as functions of shaping and profile parameters. A particularly useful form for this analysis technique is the generation of stability boundaries as measured by $\hat{s} - \alpha$ curves, which are prominently used in tokamak research, where $\hat{s}$ and α are dimensionless measures of the flux surface averaged magnetic shear and pressure gradient, respectively [1,2]. Stability curves in an $\hat{s} - \alpha$ space can be generated for the prescribed three-dimensional equilibria as well [9].

A local 3D equilibrium is given by the specification of two flux surface profile quantities, the rotational transform ι_o and the magnetic coordinate mapping $\mathbf{X}(\theta, \zeta)$ on the magnetic surface of interest $\psi = \psi_o$, where θ and ζ are any straight field line poloidal and toroidal angles. The choice of $\mathbf{X}$ is not completely free; it must satisfy constraints. The interested reader is referred to Ref. [6] for a detailed discussion of the local model. It is often convenient to specify the pressure gradient $dp/d\psi$ and the averaged magnetic shear $d\iota/d\psi$ on the surface as the two

free flux functions [2]. However, other choices are possible [6].

It is useful to distinguish $\mathbf{X}(\theta,\zeta)$ from the profiles as a fundamental way to describe the local equilibria. The choice of $\mathbf{X}(\theta,\zeta)$ and ι_o determines the magnetic field line trajectory and the magnetic surface shape in three-dimensional space. From this parametrization, one can deduce purely geometric properties of the magnetic field. In particular, the normal curvature $[\kappa_n = \hat{\mathbf{n}} \cdot (\hat{\mathbf{b}} \cdot \nabla)\hat{\mathbf{b}}]$ and geodesic curvature $[\kappa_g = \hat{\mathbf{b}} \times \hat{\mathbf{n}} \cdot (\hat{\mathbf{b}} \cdot \nabla)\hat{\mathbf{b}}]$, which play crucial roles in describing the ballooning free energy source, are derivable from the coordinate mapping [6]. Here $\hat{\mathbf{b}} = (\partial\mathbf{X}/\partial\zeta + \iota_o \partial\mathbf{X}/\partial\theta)/|(\partial\mathbf{X}/\partial\zeta + \iota_o \partial\mathbf{X}/\partial\theta)|$ and $\hat{\mathbf{n}} = (\partial\mathbf{X}/\partial\theta \times \partial\mathbf{X}/\partial\zeta)/|(\partial\mathbf{X}/\partial\theta \times \partial\mathbf{X}/\partial\zeta)|$ denote the unit directions along the magnetic field and normal to the magnetic surface, respectively. In addition, the normal torsion of the magnetic field line is also specified by $\mathbf{X}$ and given by $\tau_n = -\hat{\mathbf{n}} \cdot (\hat{\mathbf{b}} \cdot \nabla)\hat{\mathbf{b}} \times \hat{\mathbf{n}}$. The torsion is related to the local shear $s = (\hat{\mathbf{b}} \times \hat{\mathbf{n}}) \cdot \nabla \times (\hat{\mathbf{b}} \times \hat{\mathbf{n}})$ by the identity

$$s = \frac{\mathbf{J} \cdot \mathbf{B}}{B^2} - 2\tau_n , \tag{1}$$

where $\hat{\mathbf{n}} \cdot \nabla \times \hat{\mathbf{n}} = 0$ is used. Variations in the normal torsion and the Pfirsch-Schlüter current within the flux surface influence the local shear. The parallel current consistent with the quasineutrality equation is given by

$$\frac{\mathbf{J} \cdot \mathbf{B}}{B^2} = \sigma + \frac{dp}{d\psi}\lambda , \tag{2}$$

where $\sigma = \langle \mathbf{J} \cdot \mathbf{B} \rangle / \langle B^2 \rangle$ is the total flux surface averaged parallel current, $dp/d\psi$ is the pressure gradient, and the Pfirsch-Schlüter coefficient λ is determined from solutions to

$$\mathbf{B} \cdot \nabla\lambda = 2\frac{|\nabla\psi|}{B}\kappa_g , \tag{3}$$

where $|\nabla\psi|/B = |(\partial\mathbf{X}/\partial\theta \times \partial\mathbf{X}/\partial\zeta)|/|(\partial\mathbf{X}/\partial\zeta + \iota_o \partial\mathbf{X}/\partial\theta)|$ and κ_g are determined from geometric input. Equations (1)–(3) show that geometric properties dominantly describe the local shear for low current stellarators.

To consider a specific case, the $|B|$ structure of the configuration studied in the following is presumed to be dominated by a single Fourier harmonic. The practical importance of this symmetric case is that single particle orbits are integrable and hence the neoclassical transport properties of these configurations are favorable [10]. However, deviations from symmetry enhance neoclassical transport in high temperature devices. In the following, the effect of symmetry breaking contributions is shown to have important implications for ballooning stability boundaries as well.

The following parametrization is used to crudely model a quasihelically symmetric system [11] in a particular asymptotic limit. Studies of the helically symmetric experiment (HSX) indicated a low threshold for ideal ballooning instability [4]. In this approximate limit, the normal and geodesic curvatures are given by $\kappa_n \sim \cos(N\zeta - \theta)$ and $\kappa_g \sim \sin(N\zeta - \theta)$, where N denotes the toroidal periodicity. From Eq. (3), assuming $|\nabla\psi|/B \sim f(N\zeta - \theta)$ on the magnetic surface, the Pfirsch-Schlüter coefficient is dominated by the same magnetic harmonic, $\lambda \sim \cos(N\zeta - \theta)$. While the curvatures are dominated by a quasisymmetric spectrum, in general, there is no reason to believe that the normal torsion should also be quasisymmetric. The normal torsion is described by $\tau_n \sim \tau_n(N\zeta - \theta, N\zeta)$ along a magnetic field line and is field line dependent. Because of Eq. (1), this will impact the local shear and the ballooning stability properties.

As a particular example, we introduce a local helical axis configuration specified by a small number of parameters. The coordinate mapping in cylindrical coordinates is written $\mathbf{X}(\theta,\zeta) = [\mathbf{R}, \phi, \mathbf{Z}] = [\mathbf{R}(\theta, \mathbf{N}\zeta), -\zeta, \mathbf{Z}(\theta, \mathbf{N}\zeta)]$ with

$$R = R_o + \rho_o \cos\theta + \Delta\cos(N\zeta - \theta) ,$$

$$Z = \rho_o \sin\theta + \Delta\sin(N\zeta - \theta) .$$

In the asymptotic limits $N^2\Delta/R_o \gg 1 > N\Delta/R_o$, $\rho_o \ll R_o$, the helical curvature dominates the toroidal curvature, $\kappa_n \simeq -(N^2\Delta/R_o^2)\cos(N\zeta - \theta)$, and $\kappa_g \simeq -(N^2\Delta/R_o^2)\sin(N\zeta - \theta)$. For the normal torsion we include corrections due to symmetry breaking terms of order $\mathcal{O}(N\Delta/R_o)$ and find $\tau_n \simeq \iota_o/R_o - (N^3\Delta/R_o^2) \times \cos^2(N\zeta - \theta) - (N\Delta/R_o)\cos(N\zeta)$. Although the asymptotic limit studied is somewhat artificial, it does represent a particularly interesting case that allows one to identify crucial geometric information and is somewhat generic to quasisymmetric systems. An additional property, consistent with the ordering, is that the surface under investigation is stable to Mercier modes. While Mercier properties are known to influence ballooning stability in stellarators [12], we do not include it in this paper.

As in axisymmetric systems [1], ballooning theory for three-dimensional configurations relies on the use of an eikonal or WKB approach to describe the behavior on disparate length scales [13]. In particular, the linear ideal MHD perturbations are written $\Xi(\mathbf{x}) = \xi(\mathbf{x})e^{iS(\mathbf{x})/\epsilon}$, where $\epsilon \ll 1$ and the factor $S(\mathbf{x})$ satisfies $\mathbf{B} \cdot \nabla S = 0$. By using the eikonal form, the lowest order description of the mode structure is governed by the ballooning equation, which can be written, for the example equilibria, as

$$\frac{\partial}{\partial\eta}(1 + \Lambda^2)\frac{\partial\xi}{\partial\eta} + \alpha[\cos(\eta) + \Lambda\sin(\eta)]\xi = -\Omega^2(1 + \Lambda^2)\xi , \tag{4}$$

where the angle coordinate $\eta = N\zeta - \theta$ labels points along the field line,

$$\Lambda = \int_{\eta_k}^{\eta} d\eta\,[\hat{s} - \alpha\cos(\eta) + \tau_o\cos(2\eta) + \delta\cos(k\eta + k\chi)], \tag{5}$$

is the integrated local shear, $\alpha = -(dp/d\psi) \times N^2\Delta\rho_o\hat{V}'/R_o^2(N - \iota_o)^2$ is a measure of the pressure gradient, $\tau_o = N^3\Delta^2/2R_o^2(N - \iota_o)$, $\delta = N\Delta/R_o(N - \iota)$, and the factor $\hat{V}' = \oint(dl/B)\,(4\pi^2)^{-1}$ is an overall normalization factor [6]. The fact that $k = N/(N - \iota_o)$ in the last term of Eq. (5) is irrational if ι_o is irrational has implications for ballooning stability. Finally, $\chi = \theta - \iota_o\zeta$ is a field line label. The quantity $\hat{s} = (d\iota/d\psi)\,[\rho_o^2 R_o/\hat{V}'(N - \iota_o)]$ is the normalized averaged shear which is a free variable in the local equilibrium model. [Note that, from Eq. (2), one can exchange the specification of $d\iota/d\psi$ with the choice of averaged current σ_o at the surface.] With the boundary conditions $\xi = 0$ as $|\eta| \to \infty$, the ballooning equation becomes an eigenvalue equation for the normalized frequency Ω^2, with $\Omega^2 < 0$ indicating instability.

In the limit $\tau_o = \delta = 0$, the above ballooning equation is identical to the sharp boundary shifted circle equilibrium used in axisymmetric studies [1], except for the scaling factor $\iota_o/(\iota_o - N)$ multiplying the connection length that enters only into normalizing α and $\hat{s}$. In Fig. 1, the ideal ballooning stability boundaries are shown for this case with both first and second stability regions. The effect of the term proportional to τ_o alters the stability curves quantitatively; however, the same general features as the $\tau_o = 0$ case (two stability boundaries, stability at $\hat{s} = 0$) are seen since this case does not introduce symmetry breaking effects into the ballooning equation.

A more novel effect on ballooning instability is seen when the symmetry breaking contribution to the local shear as described by the term proportional to δ is present. In Fig. 1, the stability curves corresponding to nonzero δ show that there is a deterioration of the second stability regime, and for large enough δ there is only one ballooning stability boundary for a given value of $\hat{s}$. Note that ballooning instability can exist at $\hat{s} = 0$ and the variation of the local shear generally determines stability boundaries in the small $\hat{s}$ region.

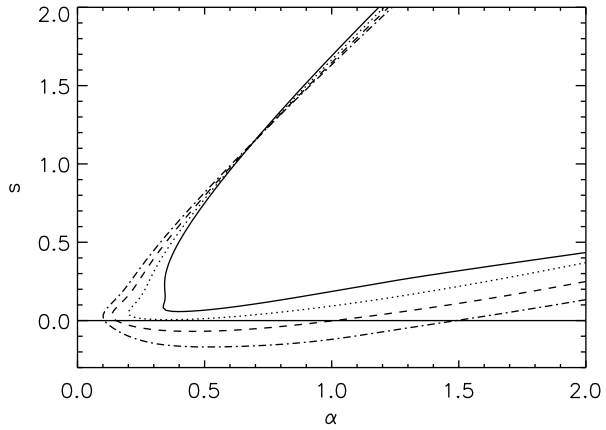

FIG. 1. Ideal MHD stability boundaries of the ballooning equation, Eq. (4), with $\tau_o = 0$, $k = \pi^2/8$, and $\chi = 0$ with different values of the symmetry breaking factor δ. The solid, dotted, dashed, and dash-dotted curves correspond to $\delta = 0$, 0.15, 0.30, and 0.45, respectively.

The effect of incommensurate helicities in three-dimensional equilibria has been studied by Cuthbert and Dewar [14]. They point out that, when incommensurate helicities are present, ballooning mode eigenfunctions can be localized along the magnetic field lines even when $\hat{s}$ is small. This behavior resembles the Anderson localization process [15] of solid state physics, where electron transport is inhibited by localized electron wave functions due to the presence of impurities on a periodic lattice. In Fig. 2, plots of the ballooning mode eigenfunctions corresponding to that obtained with the same values of α and $\hat{s}$, but with varying levels of δ, demonstrate the localizing effect of the symmetry breaking term in the local shear.

A considerable amount of work in the stellarator community has been spent on three-dimensional configurations with quasisymmetry since the predicted neoclassical transport at high temperature is considerably better than conventional stellarators [10]. In quasisymmetry systems, a prominent harmonic dominates the magnetic field spectrum and hence the components of the curvature and Pfirsch-Schlüter spectrum. However, these approaches do not address the symmetry properties of the local shear, which we show can have dramatic consequences for ideal ballooning stability. In particular, for the standard configuration discussed in Ref. [4], the stability curves, as calculated using the technique of Ref. [9] and shown in Fig. 3, are qualitatively similar to the academic example of Fig. 1. In both cases, there are instability regions that cross $\hat{s} = 0$ and a corresponding loss of "second stability." The region in profile space with small $\hat{s}$ is of considerable practical applicability for many stellarator applications. An important conclusion from this paper is that the helical content of the local shear determines ballooning stability boundaries in this regime.

The stability boundaries as deduced from solutions to Eq. (4) are often used to predict stable operating regimes

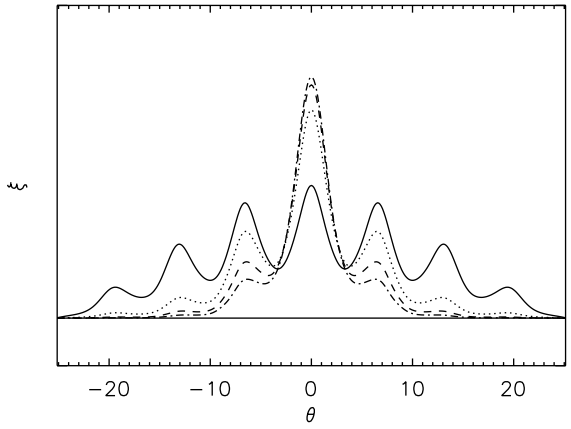

FIG. 2. The ballooning mode eigenfunctions for $\alpha = 0.5$ and $\hat{s} = 0.05$ for varying values of δ. The solid, dotted, dashed, and dash-dotted curves correspond to $\delta = 0$, 0.15, 0.30, and 0.45, respectively. For higher values of δ, the ballooning eigenfunctions are more localized along the field line and the growth rates increase.

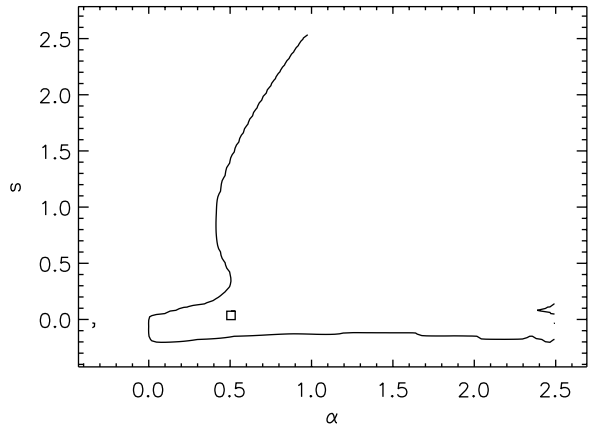

FIG. 3. The stability boundaries constructed for the standard HSX configuration studied in Ref. [4]. The plot is constructed by fixing the magnetic geometry and allowing the two profile functions to vary at the magnetic surface following the prescription of Ref. [9]. The box indicates the position in profile parameter space of the initial equilibrium.

in magnetic configurations. However, Eq. (4) describes only the leading order solution to the linearized ideal MHD equations using the ratio of the disparate length scales as an expansion parameter. To completely specify the mode structure, one must examine the next order solution which introduces a second eigenvalue problem for the global solution. In axisymmetric systems, the next order solution is integrable and the resultant eigenvalues can be related to the eigenvalues of the local solutions [1]. In three-dimensional equilibria, the higher order solution is nonintegrable in general and constructions of the global solutions are problematic [13]. Since the stability boundaries in Fig. 1 are dependent upon three-dimensional geometric effects, one might speculate that these limits are overly pessimistic.

In this Letter, we point out the importance of the symmetry breaking effects of the local shear on the ideal MHD ballooning stability properties. Using a recently developed technique for generating sequences of local three-dimensional equilibria which allows for easy manipulation of 3D shaping and profile plasma profiles, one is able to create generalized $\hat{s} - \alpha$ plots for generic equilibria showing stability boundaries as functions of equilibrium parameters. The work suggests that, generically, the presence of symmetry breaking components in the local shear of quasisymmetric configurations can reduce ideal MHD stability threshold conditions and eliminate second stability regimes. For particular configurations, one needs to perform more quantitative calculations for instability threshold predictions. However, one can hopefully use the understanding developed here to construct more robustly stable stellarator configurations.

The authors thank Professor Robert Dewar and Professor J. D. Callen for useful discussions. This work is supported by the U.S. Department of Energy under Contract No. DE-FG02-99ER54546.

[1] J. W. Connor, R. J. Hastie, and J. B. Taylor, Phys. Rev. Lett. **40**, 396 (1978).
[2] J. M. Greene and M. S. Chance, Nucl. Fusion **32**, 453 (1981).
[3] W. A. Cooper *et al.,* in *Proceedings of the 19th European Physical Society Conference on Controlled Fusion and Plasma Physics, Innsbruck, 1992* (European Physical Society, Petit-Lancy, Switzerland, 1992), Vol. 10C, p. 557; R. Moeckli and W. A. Cooper, Nucl. Fusion **33**, 1899 (1993); W. A. Cooper and H. J. Gardner, Nucl. Fusion **34**, 729 (1994); R. Moeckli and W. A. Cooper, Phys. Plasmas **1**, 793 (1994).
[4] J. A. Talmadge and W. A. Cooper, Phys. Plasmas **3**, 3713 (1996).
[5] D. Lortz and J. Nuhrenberg, Phys. Lett. **68A**, 49 (1978).
[6] C. C. Hegna, Phys. Plasmas **7**, 3921 (2000).
[7] C. Mercier and N. Luc, Commission of the European Communities, Brussels, Report No. EUR- 5127e 140, 1974.
[8] R. L. Miller, M. S. Chu, J. M. Greene, Y. R. Lin-Liu, and R. E. Waltz, Phys. Plasmas **5**, 973 (1998).
[9] C. C. Hegna and N. Nakajima, Phys. Plasmas **5**, 1336 (1998).
[10] A. H. Boozer, Phys. Fluids **23**, 904 (1980); Phys. Fluids **24**, 1999 (1981).
[11] J. Nührenberg and R. Zille, Phys. Lett. **114A**, 129 (1986).
[12] N. Nakajima, Phys. Plasmas **3**, 4545 (1996); Phys. Plasmas **3**, 4556 (1996).
[13] R. L. Dewar and A. H. Glasser, Phys. Fluids **26**, 3038 (1983).
[14] P. Cuthbert and R. L. Dewar, Phys. Plasmas **7**, 2302 (2000).
[15] P. W. Anderson, Phys. Rev. **109**, 1492 (1958).